Enhanced Relativistic Electron-Beam Deposition

M. M. Widner and J. W. Poukey
Plasma Theory Division, Sandia Laboratories, Albuquerque, New Mexico 87115

and

J. A. Halbleib, Sr.
Theoretical Division, Sandia Laboratories, Albuquerque, New Mexico 87115
(Received 12 November 1976; revised manuscript received 10 January 1977)

A two-dimensional electron transport model is used to study relativistic electron-beam (REB) deposition in thin metal anodes in the presence of strong, macroscopic electric and magnetic fields. Enhancement in power per mass deposited is calculated under certain conditions for high-current beams, which has important implications for REB fusion. Requirements for enhanced deposition are discussed, and a possible diode design is given.

Calculations of beam requirements for relativistic electron-beam (REB) driven fusion targets indicate that from 8×10^{14} to 3.6×10^{14} W of deposited power is needed for achieving breakeven.[1,2] The target radius and shell thickness are largely determined by the electron penetration depth in the material and the specific power deposited (power per mass) in the target shell. As has been postulated,[3] if there were some means of reducing the electron penetration depth and/or enhancing the specific power deposited, then the beam requirements could be relaxed, since targets with less mass could be used. Several methods of obtaining deposition enhancement have been proposed and include magnetic stopping in macroscopic B fields,[3-6] scattering from micromagnetic turbulence,[7] electrostatic reflexing,[8-10] and beam stagnation.[11]

We present here calculations of electron deposition in thin, planar Au foils, specifically investigating the effects of the electric and magnetic fields on the deposition. The examples considered are for beam conditions of the HYDRA accelerator[12] (800 kV, 250 kA, 80 nsec).

The electron-transport calculations involve a collisional Monte Carlo model similar to that developed by Berger.[13] Energy loss is accounted for in the continuous-slowing-down approximation[14] (CSDA) and the theory of Goudsmit and Saunderson[15] is used to describe multiple elastic scattering. Macroscopic electric and magnetic forces, which are not self-consistent with the particle motion, act on the particles between scattering events. The model here was previously reported[16] and is similar to the model of Zinamon, Nardi, and Peleg.[17] Comparison calculations with a more recent version of the model of Ref. 6 have given good agreement using 1600 histories per deposition calculation.

Figure 1 plots specific power deposited in the focal region P_s (W/g) vs foil thickness $\rho\Delta$ (g/cm^2) of a planar Au foil for a variety of beam and field conditions. The current-density profile $J(r)$ (A/cm^2) is chosen to be a truncated Gaussian profile, i.e., $J(r)=J_0\exp(-r^2/a^2)$ for $r<r_b$ and $J(r)=0$ for $r\geq r_b$, where $J_0=$const, $a\approx1.20r_b$, and $r_b=$beam radius $[J(r_b)=J_0/2]$. The beam density is assumed proportional to J. We define P_s as the deposited power within $r<r_b$, divided by the focal mass $M=\rho\Delta\pi r_b^2$. Since, for the cases of interest, significant target expansion occurs on the time

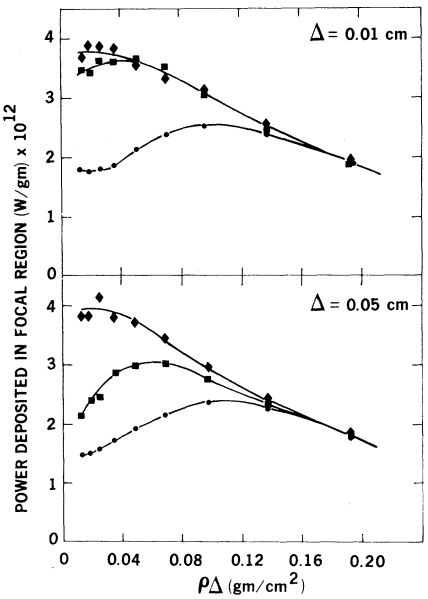

FIG. 1. Specific power deposited in the focal region vs a real foil density $\rho\Delta$. The symbols represent the following: (◇) B fields in the diode, foil, and behind the foil; (□) B fields in the diode and behind the foil; and (○) B fields in the diode only.

scale of the REB pulse duration, expanded foils are considered with thicknesses $\Delta = 0.01$ cm (upper graph) and $\Delta = 0.05$ cm (lower graph). In both cases a uniform foil density ρ is assumed. We further consider an azimuthal magnetic field B consistent with $J(r)$; and we chose $r_b = 0.2$ cm. An axial electric field $E_z = 10^6$ V/cm is assumed in the diode region while $E_z = 0$ (i.e., charge neutralization) within and behind the foil. Electrons are launched on the front surface of the foil with isotropic incidence. Finally, we consider the three extreme cases of B penetration: (1) B only in the diode region; (2) B in the diode region and the region behind the foil; and (3) B in the diode, the foil, and the region behind the foil. The particle energy is $V = 800$ kV and the total pinch current $I = 90.6$ kA within r_b giving $J_0 = 10^6$ A/cm^2.

As can be seen in Fig. 1, for $\rho\Delta \lesssim 0.1$ enhancement of P_s occurs for the cases with B either on both sides of the foil and/or in the foil (the upper curves in each respective graph) over those with diode B only (lower curves). This $\rho\Delta$ condition is equivalent to a collisionless condition for the beam electrons which, for the case of B penetration from the diode, is $\rho\Delta < (\rho l)_s$ for $\Delta < r_L$ or $\rho r_L < (\rho l)_s$ for $\Delta > r_L$; where $(\rho l)_s = 4.13 A\gamma^2\beta^4/Z^2 \ln\Lambda$ (g/cm^2) = the 90° deflection length,[3] A is the atomic mass (amu), Z the atomic number, $\gamma = 1 + V(5.11\times10^5)^{-1}$, V = diode voltage (V), $\beta = (1 - 1/\gamma^2)^{1/2}$, Λ the ratio of maximum to minimum scattering angle, and r_L = Larmor radius (cm) for a beam electron in an "average" B field. For the case where B is on either side of the foil, but not in the foil, the condition is again $\rho\Delta < (\rho l)_s$. For the conditions of Fig. 1, $(\rho l)_s \cong 0.062$ for $\ln\Lambda = 10$. Other relevant lengths are the CSDA range ≈ 0.58 g/cm^2 and the practical range (the depth at which most of the energy is deposited) $= R_p \approx 0.19$ g/cm^2. For $\rho\Delta > R_p$, there is little enhancement.

We have also performed P_s vs $\rho\Delta$ calculations (not shown) for unexpanded foils ($\rho = 19.3$) in the range $\rho\Delta \geq 0.01$. Agreement within ~10% with the curves in Fig. 1 with $\Delta = 0.01$ is observed. Another feature of Fig. 1 is that as $\rho\Delta \to 0$, with diode B only, we approach the thin stopping power limit $P_s = I(\mathrm{A}) \times \rho^{-1}\partial E/\partial x(\mathrm{V\ cm^2/g})/\pi r_b^2 \cos\theta = 1.68 \times 10^{12}$, where θ = average angle of incidence = 60° for anisotropic distribution. Also seen in Fig. 1 is the reduction in enhancement for the expanded target $\Delta = 0.05$ cm over that for $\Delta = 0.01$ for the case with B in the diode and behind the foil. This is a result of electrons exciting the focal volume radially due to their initial angular spread and to scattering.

A second condition for enhanced deposition due to B fields is either (1) the presence of the B field to at least a depth of r_L in the material ($r_L < \delta$, where δ is the resistive skin depth) or (2) the presence of B in front and back of the foil. Implicit to this first case is the requirement that the magnetic Reynolds number is small, $R_m = 1.26\times10^{-8}\sigma v_{\mathrm{exp}} r_L \ll 1$, where σ = material conductivity (mho/cm) and v_{exp} = expansion velocity (cm/sec). The second case requires a region with no current neutralization behind the foil.

We should also note that for the cases of field penetration, while P_s is large for thin foils ($\rho\Delta \sim 0.02$), the fraction of the total power deposited is small ~12% with the remaining power being carried primarily by transmitted electrons. The transmitted electrons are found to have a large velocity component $v_\parallel$, parallel to B_θ, and drift in the $+z$ direction (the beam direction) as a result of centrifugal forces. The ∇B drift, on the other hand, requires large $v_\perp$ and is in the $-Z$ direction (opposite the beam direction) for $r < r_b$. The transmission loss for $r < r_b$ can thus be thought of as beam electrons scattering in the foil into a "loss cone" in velocity space ($v_\parallel \gtrsim \sqrt{2}\, v_\perp$).

Estimates of deposition enhancement can be made by noting

$$\tilde{P}_s = \tilde{I}(\rho^{-1}\partial E/\partial x)\rho x/\rho\tilde{\Delta}S,$$

where $\tilde{P}_s$ is the local specific power deposited, $\tilde{I}$ is the current incident on area S, ρx the areal density along the electron path (counting multiple passes), and $\rho\tilde{\Delta}S$ the mass of the material volume. In the limit as x and $\tilde{\Delta} \to 0$, this becomes

$$\tilde{P}_s = (x/\tilde{\Delta})J\rho^{-1}\partial E/\partial x,$$

and for straight, normal paths ($x = \tilde{\Delta}$) we recover the thin stopping limit. The simplest physical interpretation of the deposition enhancement is that it results from an increased particle path length ($x > \tilde{\Delta}$) within the material, due to the gyromotion of the particle. A more quantitative definition is to note that $x/\tilde{\Delta} = fv/u_D$, where f is a factor of order unity, v is the electron speed, and u_D the drift velocity component normal to the incremental area S defined above. For the problem we are considering, we can show that the enhancement $v/u_D \propto I/I_A$, for $I > I_A$, where $I_A = 17\,000\beta\gamma$ and where u_D is given by centrifugal and ∇B drifts. Thus we would expect $P_s \propto I^2$, provided $P_s \ll P_{\max} = VI/M$.

To test this hypothesis we vary I holding other parameters fixed—$\rho\Delta = 0.017\,06$, $\Delta = 0.01$, $V = 0.8$

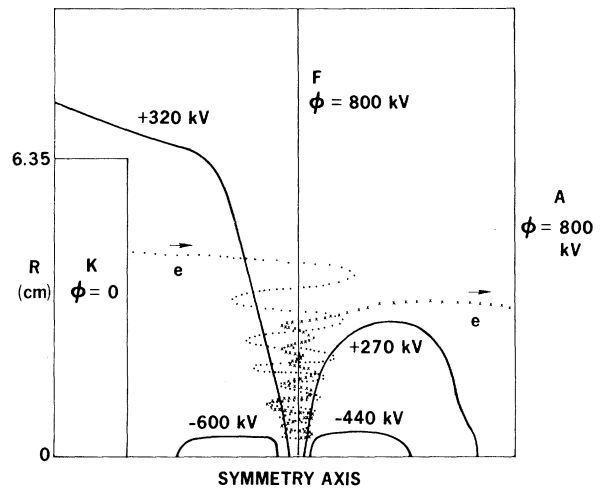

FIG. 2. Computer simulation of an 800-kV, 250-kA reflex-pinch HYDRA diode, showing several equipotentials and one electron (e) orbit. Dots show electron position moving towards axis, ×'s show electron position moving away from axis. Self-magnetic field is perpendicular to plane of figure. Cathode radius is 6.35 cm, total A-K gap is 1.2 cm.

MeV, truncated Gaussian beam and current-density profile with $r_b = 0.2$ cm, penetrating B fields, and isotropic incidence. We find that for $I \sim 10^5$ A, $P_s \propto I^2$ and that $P_s \ll P_{\max}$. In the range of $I \gtrsim 5\times10^5$ A $P_s \propto I$ since the beam is being depleted, i.e., $P_s \to P_{\max} = 3.73\times10^8 I$. As the fraction of the beam deposited becomes large, however, the assumed B on the back side of the foil is not consistent with the transmitted current.

A way in which a diode might be constructed to achieve enhanced deposition is shown in Fig. 2. A 6.35-cm-radius, flat-faced cylindrical HYDRA cathode (K) is placed close to a flat anode (A), and a thin foil (F) (also at anode potential) is placed between. The cathode may be the leading edge of an expanding plasma. For the case of Fig. 2, V is 800 kV and the current reaching the anode is 250 kA. The solution was obtained using the steady-state diode code,[18] assuming no ion flow, and no space charge neutralization in either the K-F or F-A gap. In this "reflex-pinch" configuration the electrons drift radially toward the axis making an average of about twenty foil crossings per particle. Note that the negative potential "hills" on each side of the foil near the axis "trap" the electrons between them, and cause a reflection in radial velocity. No electrons cross the F-A gap near the axis, so the electrons reaching the anode are not pinched. Both scattering and energy loss are neglected in this diode calculation, which should be valid for $N\rho\Delta/\cos\alpha \ll (\rho l)_s$, where N is the number of passes and α an average angle of incidence on the foil. The electron density is peaked near the axis at the foil.

The solution shown in Fig. 2 will not persist indefinitely, because as the foil is heated adsorbed gases will be released, a plasma will form, and ions will be emitted. The time for ion flow to begin will depend on the properties of the foil, but will probably be a few tens of nanoseconds at most. We repeated the calculation including space-charge–limited ion emission in both directions from the foil. As expected,[18] the ions cause the electrons to pinch substantially in the K-F gap. As suggested by a number of workers, this indicates that foils or injected plasma can be used to decrease the pinch formation time in large diodes. The well depth, particularly in the F-A gap, is decreased, and the average number of foil crossings per electron is about half, compared to the no-ions case. The electron current is reduced somewhat, but because of the pinching the electron energy will now be deposited in a smaller area of the foil; the electron (and ion) density is still peaked on axis.

In summary, we have studied enhanced REB deposition in thin foils resulting from macroscopic electric and magnetic fields. The conditions necessary for magnetically enhanced deposition include the following: (1) that the beam electrons are collisionless, (2) the presence of B either to the depth of at least r_L in material or on either side of the foil, and (3) a sufficiently high current beam such that $v/u_D > 1$. Calculations indicate that the enhancement is proportional to I/I_A, for $I > I_A$ with the deposited power given approximately as $P_s \approx (I/I_A)(I/\pi r_b^2)\rho^{-1}\partial E/\partial x$, for $P_s < VI/M$. Magnetically enhanced deposition should thus become increasingly important for higher-current beams. We have seen that an interesting diode configuration for obtaining enhanced deposition is the "reflex-pinch." Future studies are underway to assess more carefully the role of self-consistent beam and diode electric and magnetic fields.

The authors would like to thank Dr. F. C. Perry, Dr. M. J. Clauser, Dr. J. R. Freeman, Dr. G. Yonas, and Dr. A. J. Toepfer for helpful discussions.

[1]M. J. Clauser, Phys. Rev. Lett. 34, 570 (1975).
[2]M. A. Sweeney and M. J. Clauser, Appl. Phys. Lett. 27, 483 (1975).

[3]G. Yonas, J. W. Poukey, K. R. Prestwich, J. R. Freeman, A. J. Toepfer, and M. J. Clauser, Nucl. Fusion 14, 731 (1974).
[4]F. Winterberg, Nucl. Fusion 12, 353 (1972).
[5]J. Chang *et al.*, in *Proceedings of the Fifth International Conference on Plasma Physics and Controlled Nuclear Fusion Research, Tokyo, Japan, 1974* (International Atomic Energy Agency, Vienna, Austria, 1975).
[6]J. A. Halbleib, Sr., and W. H. Vandevender, IEEE Trans. Nucl. Sci. NS-22, 2356 (1975).
[7]D. A. Tidman, Phys. Rev. Lett. 35, 1228 (1975).
[8]S. Humphries, Jr., R. N. Sudan, and W. C. Condit, Jr., Appl. Phys. Lett. 26, 667 (1975).
[9]D. S. Prono, J. M. Creedon, I. Smith, and N. Bergstrom, J. Appl. Phys. 46, 3310 (1975).
[10]S. A. Goldstein and J. Guillory, Phys. Rev. Lett. 35, 1160 (1975).
[11]M. J. Clauser, M. A. Sweeney, and A. V. Farnsworth, Jr., in IEEE International Conference on Plasma Science, Austin, Texas, May 1976 (unpublished), Paper 6A3.
[12]T. H. Martin, IEEE Trans. Nucl. Sci. NS-20, 289 (1973).
[13]M. J. Berger, *Methods in Computational Physics* (Academic Press, New York, 1963), Vol. I, p. 135.
[14]F. Rohrlick and B. C. Carlson, Phys. Rev. 93, 38 (1954).
[15]S. Goudsmit and J. L. Saunderson, Phys. Rev. 57, 24 (1940).
[16]M. M. Widner and J. A. Halbleib, Sr., Bull. Am. Phys. Soc. 20, 1272 (1975).
[17]Z. Zinamon, E. Nardi, and E. Peleg, Phys. Rev. Lett. 34, 1262 (1975).
[18]J. W. Poukey, J. Vac. Sci. Technol. 12, 1214 (1975).

Theory of Turbulence in Superfluid ^{4}He

K. W. Schwarz
IBM Thomas J. Watson Research Center, Yorktown Heights, New York 10598
(Received 2 December 1976)

A consideration of the dynamics of a vortex tangle leads to a new equation describing turbulence in superfluid helium. The equation is seen to be remarkably successful in predicting the steady-state properties of dissipative counterflow.

At sufficiently small velocities, superfluid helium will flow through a channel without any measurable dissipation. Above certain critical velocities, however, dissipative behavior sets in as small amounts of quantized vortex line grow by interacting nonconservatively with the normal fluid and with the walls of the channel. Although interest has centered primarily on the critical velocities themselves, numerous experiments have also been performed to study the turbulent state generated when the superfluid is driven far into the dissipative regime.[1-5]

It was suggested by Vinen in his admirable papers on the subject that steady-state superfluid turbulence will consist of a random tangle of quantized vortex lines maintained in equilibrium by competing growth and annihilation processes. He proposed an equation governing the total line length L per unit volume in the presence of counterflowing normal and superfluid velocity fields $\vec{U}_n$ and $\vec{U}_s$. Although this equation has proved extremely useful, it is essentially phenomenological in character. That is, the theoretical arguments which were used to derive the Vinen equation were based on a number of erroneous premises, the most important of which was that the important characteristic velocity acting on the vortex tangle is the random interline velocity.

Our purpose here is to present a new theory of superfluid turbulence, obtained by considering the actual dynamics of a vortex tangle. The predictions of the theory are compared with the determination by Vinen[1] of L as a function of $U_n - U_s$ and T, and the recent measurements by Ashton and Northby[5] of the average drift velocity of the vortex tangle. Additional calculations, as well as details of the derivation and of the numerical integration technique, will be given in later papers.

The vortex tangle must be treated in some approximate statistical fashion. If we describe the vortex line by the parametric form $\vec{r}(s,t)$, the local self-induced velocity $\partial\vec{r}(s,t)/\partial t$ measured with respect to U_s is given by[6]

$$\vec{v}_1 = -(\kappa/4\pi)\vec{r}'\times\vec{r}''[\ln(ar'')+O(1)], \qquad (1)$$

where primes denote differentiation with respect to the arc length s, $r'' = |\vec{r}''|$, κ is the quantum of circulation, a is the core cutoff parameter, and $O(1)$ represents nonlocal corrections of order 1. Since the behavior of a local line element is determined primarily by this velocity, we characterize the vortex tangle in terms of a distribution in $\vec{v}_1$, or, equivalently, a distribution in $\vec{v}_1/v_1$ and the local radius of curvature $R = (r'')^{-1}$. Although it seems to be a reasonable simplification to con-